technologies

MDPI

*Article*

# A Framework for Distributed Orchestration of Cyber-Physical Systems: An Energy Trading Case Study

**Kostas Siozios**

Department of Physics, Aristotle University of Thessaloniki, 54636 Thessaloniki, Greece; ksiop@auth.gr

**Abstract:** The increasing number of active energy consumers, also known as energy prosumers, is dramatically changing the electricity system. New products and services that adopt the concept of dynamic pricing are available to the market, where demand and price forecasting are applied to determine schedule loads and prices. Throughout this manuscript, a novel framework for energy trading among prosumers is introduced. Rather than solving the problem in a centralized manner, the proposed orchestrator relies on a distributed game theory to determine optimal bids. Experimental results validate the efficiency of proposed solution, since it achieves average energy cost reduction of 2×, as compared to the associated cost from the main grid. Additionally, the hardware implementation of the introduced framework onto a low-cost embedded device achieves near real-time operation with comparable performance to state-of-the-art computational intensive solvers.

**Keywords:** distributed decision making; dynamic energy pricing; game theory; hardware implementation; low complexity



**Citation:** Siozios, K. A Framework for Distributed Orchestration of Cyber-Physical Systems: An Energy Trading Case Study. *Technologies* **2024**, *12*, 229. https://doi.org/10.3390/technologies12110229

Academic Editor: Dongran Song

Received: 26 October 2024
Revised: 6 November 2024
Accepted: 11 November 2024
Published: 13 November 2024



## 1. Introduction

The growing emphasis on energy efficiency, coupled with the proliferation of renewable energy sources and the advent of smart-grid technologies, signifies a paradigm shift in the energy landscape. Buildings are poised to transcend their traditional role as passive consumers and emerge as active participants in the energy market. This evolution will give rise to autonomous micro-grids equipped with energy trading capabilities and the flexibility to dynamically manage electrical loads. This transition is already evidenced by the emergence of innovative utility programs, such as market-driven pricing, which empower end users to optimize their energy consumption patterns. By replacing conventional flat rates with dynamic pricing models, where the cost per kilowatt-hour (kWh) fluctuates based on temporal factors, weather conditions, and grid demand, consumers are incentivized to actively participate in grid balancing and efficiency efforts [1]. This paradigm shift not only benefits individual consumers but also contributes to a more robust and sustainable energy ecosystem.

Dynamic pricing, enabled by advanced trading mechanisms, empowers both energy producers and consumers to actively engage in the electricity market. By leveraging fluctuating prices that reflect real-time demand, this demand-side management strategy fosters a more efficient and responsive energy system. While the concept has generated considerable interest within academic circles, widespread implementation has been hampered by technological and regulatory hurdles, resulting in reticence among energy suppliers and policymakers [2]. Moreover, both producers and consumers remain apprehensive about embracing dynamic pricing. This hesitancy stems from the inherent uncertainties associated with this novel paradigm, where potential benefits are coupled with financial risks. To fully realize the potential of dynamic pricing and alleviate these concerns, sophisticated frameworks are essential. These frameworks must effectively address real-time operational constraints, including mitigating generation variability and accommodating fluctuations in energy consumption patterns [3].

The emergence of peer-to-peer (P2P) energy trading represents a paradigm shift in energy distribution and market dynamics, aligning with the broader trend of decentralized energy systems [4]. This innovative approach empowers individuals, termed "prosumers", to engage directly in energy exchange, fostering localized energy communities and promoting greater autonomy and resilience within the energy landscape. Numerous P2P energy trading initiatives have been implemented, with projects such as Piclo, Vandebron, and PeerEnergyCloud demonstrating successful engagement of thousands of prosumers [5]. These initiatives encompass a spectrum of operational models. Some prioritize the development of sophisticated business models and platforms that function akin to traditional energy suppliers within the existing market framework. Others emphasize localized energy management through advanced algorithms and systems integrated within micro-grids, facilitating enhanced control and optimization at the community level. This diversity underscores the inherent versatility of P2P energy trading and its capacity to accommodate diverse market structures and consumer preferences, driving innovation and competition within the evolving energy sector.

The ongoing evolution of complex systems is characterized by a pronounced shift towards computational intelligence, diminishing the reliance on direct human intervention. This trajectory, in synergy with rapid advancements in sensing, measurement, process control, and communication technologies, has culminated in the emergence of cyber–physical systems (CPSs), as depicted in Figure 1. More specifically, the exceptional capabilities of CPS are poised to revolutionize the design and development of next-generation engineering platforms, as these platforms will exhibit unprecedented levels of autonomy, functionality, and usability, far surpassing the capabilities of contemporary systems. Notwithstanding their transformative potential, the design and implementation of CPSs presents formidable challenges. The inherent complexity arises from the imperative to seamlessly orchestrate a multitude of heterogeneous components and services. This intricate orchestration often necessitates the utilization of high-performance computing (HPC) or cloud infrastructures. However, the realization of ubiquitous CPS adoption hinges critically on the development of frameworks that can be efficiently deployed even on resource-constrained platforms. This challenge is further magnified when real-time operational constraints are imposed on the target system, demanding innovative and highly efficient decision-making mechanisms.

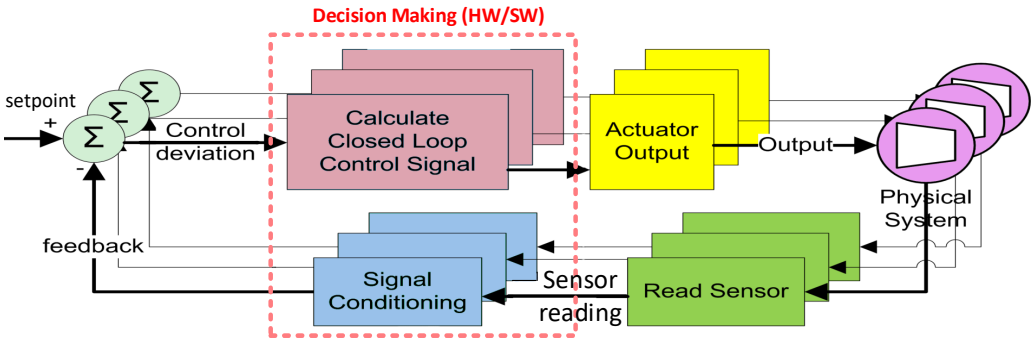


**Figure 1.** Functionality of a cyber–physical system.

While both CPS and closed-loop control systems blend physical processes with computational algorithms, creating a dynamic interplay where the digital realm senses, analyzes, and influences the physical world, they differ significantly in scope and complexity. At their core, both utilize feedback mechanisms. Sensors embedded in the physical environment provide data to computational units, which in turn, process this information and generate commands for actuators to effect changes in the physical system. This creates a continuous loop of sensing, processing, and actuation, enabling dynamic responses to changes in the physical environment. However, CPSs distinguish themselves through their broader scope and heightened complexity. While a closed-loop control system might focus on a specific, localized task, a CPS extends this concept to encompass intricate networks

of interconnected devices, distributed computing architectures and interactions between heterogeneous components.

Furthermore, CPSs often incorporate human factors into their design, recognizing that human interaction and decision making play a crucial role in many applications. This human-in-the-loop paradigm differentiates CPSs from traditional closed-loop control systems, which may operate autonomously with minimal human intervention. CPSs might, for instance, provide operators with real-time information and decision support tools, allowing them to supervise and intervene in the system's operation when necessary. This integration of human intelligence with computational capabilities allows CPSs to tackle complex scenarios that require both automated control and human oversight.

Finally, CPSs often exhibit adaptive and learning capabilities, enabling them to dynamically adjust their behavior based on accumulated experience and evolving environmental conditions. This contrasts with closed-loop control systems, which typically adhere to a predetermined control strategy. Through machine learning algorithms and data analytics, CPSs can continuously refine their models, optimize their performance, and adapt to unforeseen circumstances. This adaptability is essential for CPSs operating in dynamic and unpredictable environments, where pre-programmed rules may prove insufficient to ensure optimal performance (Table 1).

**Table 1.** Symbols.

| Symbol | Description |
|---|---|
| $M$ | Number of distributed energy prosumers |
| $E_i^D$ | Expected energy loads for prosumer $i$ |
| $E_i^{RS}$ | Energy generation forecast for prosumer $i$ |
| $E_i^{PV}$, $E_i^W$ | Energy generation forecast from PVs and wind turbines |
| $E_i^B$ | Current charge of prosumer $i$'s VES system |
| $E_i^{B,max}$ | Capacity of prosumer $i$'s VES system |
| $Q_i$ | Micro-grid $i$'s energy flow based on [6] |
| $Y_i$ | Forecast solar radiation and wind speed |
| $W_i$ | Observed solar radiation and wind speed |
| $M_i t$ | Current energy trading price per kWh |
| $M_i^{min}$ | Minimum reservation price for seller $i$ |
| $M_i^{max}$ | Max. reservation price for consumer $i$ |
| $AF_i^{init}$ | Initial funds for prosumer $i$ |
| $AF_i$ | Available funds for prosumer $i$ |
| $AF_i^{prv}$ | Previous value of $AF$ |
| $U_i$ | Producer's utility for selling energy budget |
| $D^{imp}$ | Main grid's flat rate |
| $D^{exp}$ | Main grid's feed-in tariff |
| $C_i$ | Cost for consumer $i$ that imports energy budget |
| $M_i^{PV}(t)$ | Market price per kWh from PV panels |
| $M_i^W(t)$ | Market price per kWh from wind turbines |
| $E_i^M$ | Overall energy traded to market from prosumer $i$ |
| $E_i^P$ | Energy that prosumer $i$ trades per auction |
| $a_i$ | Auction initiated by producer $i$ |
| $H_i$ | Max. concurrent auctions initiated by producer $i$ |
| $N$ | Total number of players per game |
| $S$ | Set of all possible strategy combinations |
| $S_i$ | Set of available strategies for player $i$ |
| $s_i^j$ | Strategy $j$ for player $i$ |
| $s$ | Strategy combination for an auction |
| $g_i$ | Total number of strategies for player $i$ |
| $P_i$ | Mixed strategy of player $i$ |
| $Z$ | Total strategy combinations per game |
| $r$ | Current round for an auction |
| $R$ | Maximum number of rounds per auction |

**Table 1.** *Cont.*

| Symbol | Description |
|---|---|
| $T_i$ | Rounds until consumer $i$ wins an auction |
| $V_i$ | Set of all the mixed strategies of player $i$ |
| $\lambda_i^k$ | Player $i$'s payoff for strategy combination $k$ |
| $B_i(r)$ | Prosumer $i$'s bid at round $r$ |
| $F_i(r)$ | Bidding aggressiveness at round $r$ |
| $\Delta B_i(r)$ | Price sensitivity for prosumer $i$ at round $r$ |

This manuscript formalizes a novel distributed orchestration framework for energy trading within micro-grids. Grounded in game-theoretic principles and a prosumer-centric architecture, the proposed solution empowers energy producers to dynamically initiate multiple auctions, fostering both cost optimization and collaborative energy sharing among prosumers. Empirical validation, leveraging diverse configurations and real-world data encompassing expected loads and energy prices, substantiates the efficacy of the framework. Notably, we observe an average energy cost reduction of 2× compared to conventional energy procurement from the main grid. Furthermore, by harnessing the inherent parallelism of low-cost embedded devices (Xilinx Zybo Z7 field-programmable gate array (FPGA) board [7]), our solution exhibits enhanced scalability and achieves near real-time execution with negligible performance degradation.

The contributions of this work are summarized as follows:

- A novel distributed orchestration framework based on game theory for energy trading within micro-grids is proposed. The introduced framework is general-purpose and can be easily refined to support the orchestration of any CPS platform.
- In contrast to conventional centralized approaches, this work proposes a fully distributed orchestration framework grounded in game theory. This inherent decentralization fosters scalability and resilience, enabling efficient management of complex interactions within the micro-grid environment.
- Experimental results, conducted with real-world data, demonstrate that our proposed solution yields substantial energy cost reductions compared to conventional energy procurement from the main grid.
- A prototype of the proposed orchestration framework was developed using hardware/software co-design techniques on a low-cost Xilinx Zybo embedded platform. The resulting solution demonstrates near-real-time operation and performance comparable to state-of-the-art model predictive control (MPC) solvers.
- To foster social cooperation among energy prosumers, our framework explores the integration of virtual energy storage (VES) systems and optimizes energy sharing strategies within the micro-grid environment. This approach facilitates collaborative energy management and enhances overall system efficiency.

The rest of the manuscript is organized, as follows: Section 2 gives an overview of relevant solutions, while the employed micro-grid's modeling is described in Section 3. The proposed framework for energy trading is introduced in Section 4. This section also explores alternative configurations towards improving the equilibrium's efficiency. Further experimental results that evaluate the efficiency of the proposed solution are provided in Section 5. Finally, Section 6 concludes the paper.

## 2. Literature Review and Motivation

The energy system is about to undergo a major transformation in the near future. In contrast to a centralized large-scale electricity generation and distribution system, a new energy landscape is emerging, where the system will be increasingly interconnected but also more decentralized. Key drivers towards this direction are the wide adoption of small-scale energy production in conjunction with the new services (e.g., dynamic pricing and energy trading) that are already available to the market.

The concept of profit maximization at Distributed Energy Resources (DERs) is addressed by several methodologies dealing with optimal decision making for the competitive environment among energy prosumers [3,8,9]. Candidate solutions towards this direction employ, among others, financial options as a tool for energy producers to hedge against generation uncertainty [10]. Additional profit is feasible with a combined and coordinated use of power from renewable sources and energy storage technologies [11]. Solutions that rely on probability distributions, such as stochastic models, are also employed to compute optimal bidding strategies for energy producers that participate in the day-ahead and adjustment markets [12]. In [13], an energy sharing model with price-based demand response is introduced and evaluated. As the actions of one influences all the others, solutions that rely on equilibrium statement, as well as the analysis of competitive situations, such as game theory or market theory, are also considered for this purpose [14,15]. In [16], different competitive and cooperative games were simulated and the results showed that it is of great benefit to cooperate, but the free-rider problem might arise. In addition, peer-to-peer (P2P) trading mechanisms were also applied to distributed energy auctions [17]. This analysis indicates that energy trading for small-scale micro-grids with DER utilization [18] is feasible [19].

Table 2 provides a qualitative comparison for representative energy trading frameworks. The majority of these solutions deal with a centralized coordination, where an independent controller is in charge of solving the optimization problem, which poses significant challenges to the concept of a CPS controlling smart grids. In detail, smart grids are inherently complex and vast, encompassing numerous interconnected devices and dynamic energy flows. Centralized control struggles to handle this scale, potentially leading to slow response times and difficulties in adapting to changing conditions. Moreover, a centralized system creates a single point of failure, leaving the entire grid vulnerable to disruptions or attacks. The real-time responsiveness required for efficient smart-grid management is hindered by the inherent latency and communication overheads of a centralized architecture. Furthermore, the diverse components and communication protocols within a smart grid demand a level of flexibility that centralized control often lacks. This rigidity can complicate the integration of new technologies and hinder seamless operation. In essence, while centralized control may seem appealing in its simplicity, it ultimately falls short of meeting the demands of a truly robust and responsive smart-grid system. This necessitates exploring more decentralized approaches that distribute intelligence and control across the grid, enabling faster response times, increased resilience, improved scalability, and enhanced privacy. While decentralized control presents its own set of challenges, it ultimately offers a more promising avenue for realizing the full potential of smart grids.

Regarding the mainstream ways of deciding upon system's selections, this is mainly performed through online [20] or MPC [21] algorithms. Although MPC for nonlinear systems has been extensively analyzed and successfully applied in various domains, it likewise encounters dimensionality issues; in most cases, predictive control computations for nonlinear real-time systems amount to numerically solving a non-convex high-dimensional mathematical problem, whose solution may require formidable computational power [22,23]. On the other hand, online algorithms exhibit limited efficiency and similar complexity compared to MPC, but they are reactive to real-time constraints. In order to manipulate the increased complexity of these algorithms, solutions that rely on heuristic methods, such as stochastic dynamic programming [24] and genetic algorithms [25], have been applied. Furthermore, in the relevant literature there are solvers for optimal decision making based on empirical models [26], simulation optimization [27], artificial neural networks (ANNs) [28], SVM classifiers [29], and fuzzy logic [30]. Although these approaches trade-off a solution's quality with the associated problem's complexity, they are rarely adopted in large-scale deployments, since their efficiency is tightly linked to excessive training and customization phases. The challenge for low-complexity solutions becomes even more important at multi-dimensional auctions, such as the one discussed

throughout this manuscript, where multiple goods (i.e., energy from multiple prosumers) are allocated simultaneously [31].

**Table 2.** Summary of recent publications for energy trading.

| References | Energy Market | Demand/ Response | Cooperative Grids | Distributed | Complexity | Customers Engagement |
|---|---|---|---|---|---|---|
| [1,32] | No | Yes | Yes | No | Low | No |
| [6] | No | Yes | No | Yes | Medium | No |
| [11,29,30] | No | Yes | No | No | Medium | No |
| [13] | Yes | Yes | No | Yes | Medium | No |
| [14–17] | Yes | Yes | No | No | High | Yes |
| [18] | Yes | Yes | Yes | No | Medium | Yes |
| [12,19,20,26–28,31] | Yes | Yes | No | No | Medium | No |
| [33] | Yes | Yes | Yes | No | Low | No |
| Framework proposed within this paper | Yes | Yes | Yes | Yes | Medium | Yes |

In addition to the aforementioned orchestrators for smart-grid environments, a burgeoning trend is the development of specialized CPS platforms explicitly tailored for this domain. This surge in development activity underscores the growing recognition of CPSs' transformative potential within smart-grid management and their capacity to address the evolving complexities of modern energy systems. Ref. [34] effectively elucidates the transformative potential of AI in reshaping power networks for a sustainable future. It explores the multifaceted ways in which AI can optimize energy generation, distribution, and consumption, while simultaneously addressing critical challenges such as grid stability and the integration of renewable energy sources. By framing this work within the broader context of "Energy 4.0", the authors underscore the increasing digitization and automation of energy systems, aligning with the tenets of Industry 4.0.

The authors of [35] provide a valuable and comprehensive overview of the Industry 4.0 paradigm. By systematically examining definitions, architectures, and recent trends, they establish a robust foundation for understanding the core principles and technological underpinnings driving this industrial transformation. The emphasis on automation and supervision systems offers a pragmatic perspective on the practical implementation and deployment of these technologies within real-world industrial environments. Similarly, the authors of [36] address the critical intersection of machine learning, cybersecurity, and smart grids. It delves into the intricate ways in which machine learning can be leveraged to enhance the security and resilience of CPSs integral to smart-grid networks. Given the increasing reliance on digital technologies within critical infrastructure, this focused examination of security is both timely and of paramount importance. Readers can anticipate gaining valuable insights into cutting-edge machine learning techniques for threat detection, anomaly identification, and proactive security measures within smart-grid environments.

Finally, the proposed CPS architecture for smart grid environments demonstrably contributes to the United Nations Sustainable Development Goal 7 (https://sdgs.un.org/goals/goal7 (accessed on 2 November 2024)) (Affordable and Clean Energy) by facilitating a transition towards a more sustainable and resilient energy ecosystem. Specifically, the system's capacity to optimize the integration of renewable energy sources, such as solar and wind power, promotes a significant reduction in reliance on fossil fuels, thereby advancing the goal of increasing clean energy utilization (SDG 7.2). Furthermore, the incorporation of advanced algorithms within the CPS architecture enhances grid efficiency through the minimization of transmission losses and the optimization of load balancing, culminating in more sustainable energy consumption patterns (SDG 7.3). Crucially, the system empowers consumers to actively engage in energy conservation efforts by providing real-time monitoring and control capabilities, thus enabling demand-side flexibility and fostering a more conscientious and efficient utilization of energy resources (SDG 7.a). By fostering the development of a smarter and more sustainable energy infrastructure, this CPS architecture

serves as a catalyst for progress towards the realization of SDG 7, ensuring universal access to affordable, reliable, sustainable, and modern energy services.

## 3. System Modeling

Figure 2 visualizes the proposed cyber–physical system (CPS), consisting of $M$ distributed energy prosumers (micro-grids) that are interconnected to the main grid with a transmission network (Table 1). Each prosumer (randomly selected among the templates depicted in Table 3) corresponds to a building that is in need of energy to operate the heating, ventilation, and air conditioning (HVAC) system, as well as nodes that generate energy. Since prosumers might generate energy from different sources (as depicted in Table 3), the overall energy generation forecast $E_i^{RS}$ is computed based on Equation (1), where $E_i^{PV}$ and $E_i^{W}$ correspond to the partial energy generated from photovoltaic panels and wind turbines, respectively. For this analysis we assume that micro-grids' PV panels and wind turbine installations generate up to 80% of the micro-grid's average daily energy loads $E_i^{D}$ (depending on the weather data), as formulated by Equation (2).

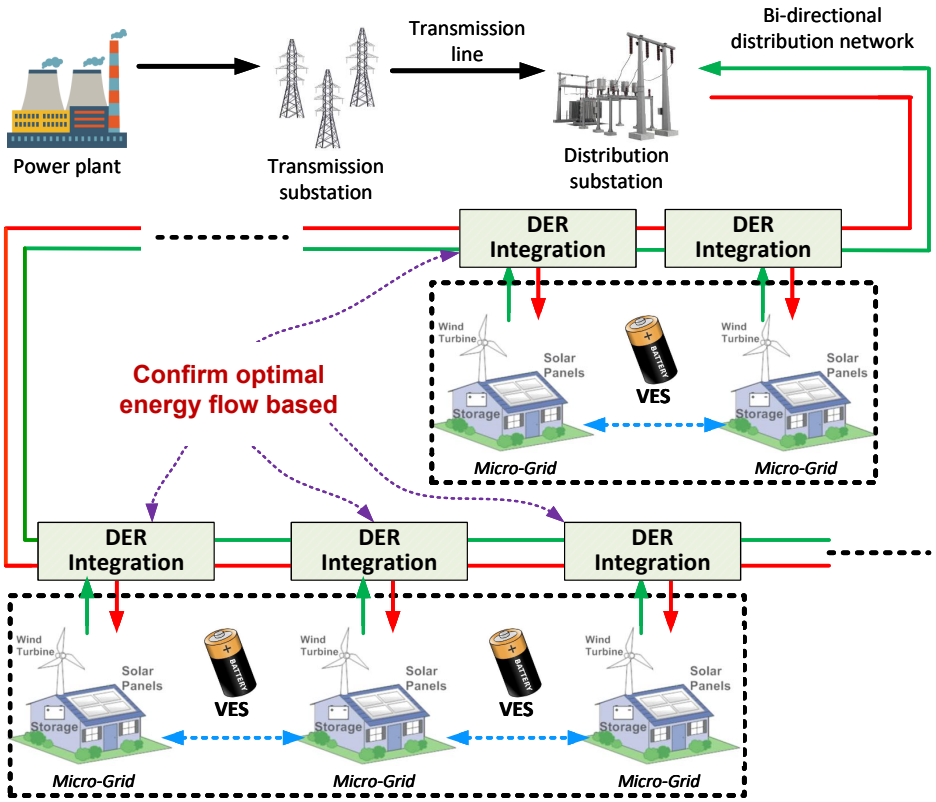


**Figure 2.** Template of our case study.

$$E_i^{RS} = E_i^{PV} + E_i^{W} \tag{1}$$

Our architectural template also enables collaborating prosumers to share energy though a common VES in order to hedge against energy generation uncertainty, variations in expected energy loads (i.e., consumption profiles), and price fluctuations. A critical parameter for the efficiency of this task is the VES's capacity $E_i^{B,max}$, which defines the maximum energy that can be stored in the VES infrastructure. Regarding our analysis, we consider that battery capacity can address 10% of the average daily expected load of the micro-grid, as calculated based on Equation (3). Also, both the micro-grid's and VES's integration to the transmission network is performed on the assumption that efficient building-to-micro-grid and micro-grid-to-grid energy flows are feasible. In order to study this parameter in detail, the proposed framework considers that a solution (auction's

outcome) is efficient if it achieves at least $Q$ = 75% of the optimal energy flow computed by [6].

$$E_i^{RS} \leq \frac{1}{365} \times \sum_{365\ days} (E_i^D) \times 80\% \tag{2}$$

$$E_i^{B,max} = \frac{1}{365} \times \sum_{365\ days} (E_i^D) \times 10\% \tag{3}$$

**Table 3.** Summary of building properties.

| Prosumer Template | Building Details | | Expected Load | Energy from Renewable Sources | Energy from Other Grids |
|---|---|---|---|---|---|
| #1 | Surface area:<br>Thermal zones:<br>Operating hours:<br>Warm-up/Pre-cool: | 350 m$^2$<br>8<br>6:00–21:00<br>No | $E_i^D$ | $E_i^{PV} \leq 80\%$ | $E_i^M \geq 20\%$ |
| #2 | Surface area:<br>Thermal zones:<br>Operating hours:<br>Warm-up/Pre-cool: | 525 m$^2$<br>10<br>8:00–21:00<br>Yes | $E_i^D$ | $E_i^{PV} \leq 60\%$<br>$E_i^W \leq 20\%$ | $E_i^M \geq 20\%$ |
| #3 | Surface area:<br>Thermal zones:<br>Operating hours:<br>Warm-up/Pre-cool: | 420 m$^2$<br>10<br>8:00–17:00<br>Yes | $E_i^D$ | $E_i^{PV} \leq 40\%$<br>$E_i^W \leq 40\%$ | $E_i^M \geq 20\%$ |
| #4 | Surface area:<br>Thermal zones:<br>Operating hours:<br>Warm-up/Pre-cool: | 280 m$^2$<br>6<br>7:00–20:00<br>Yes | $E_i^D$ | $E_i^{PV} \leq 20\%$<br>$E_i^W \leq 60\%$ | $E_i^M \geq 20\%$ |
| #5 | Surface area:<br>Thermal zones:<br>Operating hours:<br>Warm-up/Pre-cool: | 228 m$^2$<br>4<br>6:00–18:00<br>No | $E_i^D$ | $E_i^W \leq 80\%$ | $E_i^M \geq 20\%$ |

*Modeling Energy Transactions*

Let us denote by $E_i^{RS}$ the overall energy generation forecast of prosumer $i$, by $E_i^D$ the expected energy load (depending on the studied scenario, the $E_i^{RS}$ and $E_i^D$ refer to energy generation and consumption forecasts for the next day and next week), $E_i^B$ the VES's charge, and $M_i(t)$ the current energy trading price per kWh. In order to enable micro-grids to import energy from other grids, an initial amount of funds $AF_i^{init}$ is assigned to them. These funds are equal to 60% of prosumer $i$'s yearly estimated cost for HVAC operation under the optimal thermal comfort metric discussed previously and without considering any savings from renewable sources. Equation (4) formulates the initial funds assigned per prosumer, where $D^{imp}$ is the main grid's flat rate.

$$AF_i^{init} = \sum_{365\ days} \left( E_i^D \times D^{imp} \right) \times 60\% \tag{4}$$

Similarly, Equation (5) formulates the amount of energy that prosumer $i$ has to import depending on the VES's charge status. Specifically, in case $E_i^{RS}$ is not sufficient to meet prosumer $i$'s expected loads ($E_i^D$), additional energy is imported from other prosumers, or the main grid, at cost $M_i(t)$. By contrast, if the energy generation forecast exceeds the

expected loads, the spare energy is either stored to the VES (if there is enough capacity), or it is sold to other grids.

$$E_i^M = \begin{cases} \left(E_i^D - E_i^{RS} - E_i^B\right) & \text{, if } E_i^D \geq E_i^{RS} + E_i^B \\ 0 & \text{, if } E_i^D \leq E_i^{RS} + E_i^B \end{cases} \tag{5}$$

In this context, the cost and utility for prosumer $i$ who imports and exports energy in the proposed energy market are defined by Equations (6) and (7), respectively, where $D^{exp}$ is the main grid's feed-in tariff. Since prosumers might seek energy from different sources, the traded price is computed based on partial rates for electricity generation from PV panels ($M_i^{PV}(t)$) and wind turbines ($M_i^W(t)$). In such a case, the overall rate $M_i(t) = M_i^{PV}(t) + M_i^W(t)$ is computed based on Equation (8).

$$C_i = \begin{cases} \left(E_i^D - E_i^{RS} - E_i^B\right) \times M_i(t) & \text{,cost from auctions} \\ \left(E_i^D - E_i^{RS} - E_i^B\right) \times D^{imp} & \text{,cost from main grid} \end{cases} \tag{6}$$

$$U_i = \begin{cases} E_i^M \times M_i(t) & \text{,utility from auctions} \\ E_i^M \times D^{exp} & \text{,utility from main grid} \end{cases} \tag{7}$$

$$M_i(t) = \frac{E_i^{PV} \times M_i^{PV}(t) + E_i^W \times M_i^W(t)}{E_i^{PV} + E_i^W} \tag{8}$$

For this analysis we consider that energy imports/exports within the proposed electricity market are conducted at different rates, as compared to the corresponding rates from the main grid. In detail, prosumers export energy to the main grid at the feed-in tariff $D^{exp}$, which refers to the regulator's minimum guaranteed price per kWh that an electricity utility has to pay to a private, independent energy producer in the grid. Similarly, consumers import energy from the main grid at the flat rate ($D^{imp}$). On the other hand, the energy price per kWh in the proposed electricity market ($M_i(t)$) follows a more dynamic fluctuation and is computed based on the proposed game theory approach. Equation (9) formulates the increase/decrease of available funds ($AF$) for prosumer $i$ as a function of its previous value ($AF^{prv}$), when they import or export energy $E_i^M$.

$$AF_i = \begin{cases} \left(AF_i^{prv} + U_i\right) & \text{, if } E_i^{RS} \leq E_i^D \\ & \text{and spare energy is exported to other grids} \\ AF_i^{prv} & \text{, if } E_i^{RS} \geq E_i^D \\ & \text{and spare energy is stored at VES} \\ \left(AF_i^{prv} - C_i\right) & \text{, if } E_i^{RS} + E_i^B \leq E_i^D \end{cases} \tag{9}$$

Even though the proposed framework appears to exploit renewable sources as much as possible in order to minimize energy cost, this is not always the case. Specifically, uncertain parameters such as the building's dynamics, the intermittent behavior of energy generation from renewable sources, the VES' charge status, as well as the fluctuations at trading energy price cannot be considered trivial because they further complicate the problem at hand.

Finally, Figure 3 gives the simulation framework employed to compute prosumers' expected energy loads and energy generation forecast based on the EnergyPlus suite [37]. The expected energy loads per prosumer depicted in Table 3 correspond to weather and energy pricing data for optimal HVAC operation during the 52-week experiment [38,39]. This optimality refers to the maximization of occupants' thermal comfort metric according to ASHRAE standard [40,41]. Additional details about this optimality can be found in our former publication [42]. Similarly, the energy generation forecast per micro-grid is also computed with the EnergyPlus suite according to installation of PV panels and wind turbines by prosumers. Such an approach is expected to deliver more valuable insights for the occupants' energy consumption profiles, as compared to a pure statistical analysis. It is worth highlighting that the models for our simulation framework are applied with a "black-box" premise; thus, any other micro-grid, DER, or VES configuration can also be explored assuming that it is properly modeled in XML format. This feature is crucial in the CPS domain, since it enables the design, customization, and deployment of large-scale systems with increased complexity by exploiting the well established model-in-the-loop (MiL) and hardware-in-the-loop (HiL) approaches.

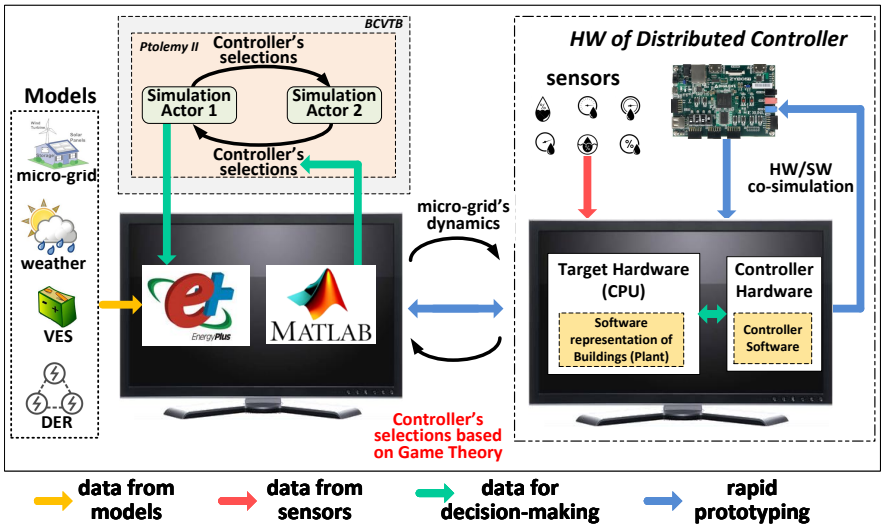


**Figure 3.** Simulation framework for supporting the proposed MiL and HiL simulations.

## 4. Proposed Framework for Supporting Orchestrator's Selections

This section introduces the proposed energy auction framework, depicted schematically in Figure 4. The auction is initiated ad hoc by energy producers in order to decide (i) to whom to sell, (ii) the amount of energy to be sold, and (iiii) the energy cost per kWh. The participants in this auction are the prosumers that are in need of energy (consumers) and seek to reduce their energy cost compared to the main grid's flat rate. The energy producer and the interested consumers act as auctioneer and bidders, respectively, for the traded $E_i^M$ energy budget. This section describes in detail the proposed framework that supports optimal energy bidding.

### *4.1. Energy Trading Based on Game Theory*

The proposed auction mechanism is realized with a game theory algorithm. Instead of relevant multi-objective optimization approaches that compute optimum (or optimal) solutions, the game theory seeks to find a Nash equilibrium, where no player has the incentive to change their offering/bidding strategy [43]. Let us consider that prosumer $i$ initiates an auction $a_i$ described by Equation (10) to sell energy budget $E_i^M$. For additional flexibility, the proposed framework enables prosumer $i$ to instantiate multiple (up to $H_i$) partial auctions, each of which trades a subset $(E_i^P)$ of the overall budget. Bidders at these auctions are prosumers that are in need of energy. The proposed solution relies on

a mixture of competitive and cooperative strategies ($S_i$) that maximize prosumers' profit ($AF_i$). In general, the prosumers are assumed to be rational decision makers, i.e., each player attempts to maximize their own utility by a set of actions in the presence of other decision makers [44].

$$Game = \left[E_i^M, S_i, \lambda_i^\nu\right], \forall i \in N \text{ and } \forall \nu \in S \tag{10}$$

where $N = \{1, 2, \ldots, n\}$ is the set of $n$ players in the game. Each of these players has to select a strategy among the available ones denoted by $s_i^{j_i}, j_i = 1, 2, \ldots, g_i$, where $g_i$ stands for the total number of strategies that player $i$ can choose. Regarding our case study, there are four valid strategies ($g_i$ = 4), which correspond to import/export energy at a given price ($s_i^1 = yes$), to decline this transaction ($s_i^2 = no$), or to come back with a lower ($s_i^3 = lower$) or higher ($s_i^4 = higher$) offer. Based on players' selections, a strategy combination consisting of $n$ elements is formed. This combination, denoted as $s \in \{(s_1^1, s_2^1, \ldots, s_n^1), (s_1^2, s_2^2, \ldots, s_n^2), \ldots, (s_1^{g_i}, s_2^{g_i}, \ldots, s_n^{g_i})\}$, refers to all the candidate strategies that players might choose in the game, where $S_i$ gives the set of player $i$'s strategies. The total number of strategy combinations in the game is computed by Equation (11).

$$Z = \prod_{i=1}^{n}(g_i) \tag{11}$$

The payoff function computes the award obtained by a single player at the outcome of a game in order to motivate players to adopt certain strategies. This payoff function for prosumer $i$ is formulated by Equation (12), where $\nu \in [1, Z]$ denotes one of the strategy combinations in $S$. The $U_i^\nu - C_i^\nu$ factor gives the profit (or cost) of energy transaction for player $i$ in strategy combination $\nu$ and $|D^\nu|$ is the absolute profit for all the energy transactions in strategy combination $\nu$. Similarly, $\gamma_i^\nu$ refers to the satisfaction level for meeting consumer $i$'s load forecast in strategy combination $\nu$. Finally, $\pi$ is a small positive number in order to guarantee that the denominator is not zero. Such a function ensures that the higher the payoff value $\lambda_i^\nu$ is, the better the outcome of strategy combination $\kappa$ is recognized to be by player $i$. Based on this function it is also possible to compute player $i$'s payoff $\lambda_i(S)$ for a strategy combination $S$.

$$\lambda_i^\nu = \frac{(U_i^\nu - C_i^\nu) \times \gamma_i^\nu}{|D^\nu| + \pi} \tag{12}$$

Next, we discuss further the three factors that define player $i$'s payoff in strategy combination $\nu$:

- $U_i^\nu - C_i^\nu$: Since prosumers import and export energy, both utility and cost factors are considered. The higher value for this factor denotes the benefit for energy prosumers in terms of improving the $AF$ metric and the higher possibility there is that player $i$ can export additional energy (or import less energy) to/from other prosumers. This factor also considers the renewable source of the traded energy, as PV panels and wind turbines lead to different costs (based on $M_i^{PV}(t)$ and $M_i^W(t)$ rates). Therefore, $U_i^\nu - C_i^\nu$ is placed in the numerator so that the higher value, the higher $\lambda_i^\nu$ is.
- $\gamma_i^\nu$: It is placed in the numerator as a multiplier and takes a binary value (either 0 or $\pm 1$) following this principle: if the strategy chosen by a player $i$ satisfies the consumer's expected energy loads, $\gamma_i^\nu$ takes the value of $\pm 1$ to approve the current strategy and return a positive numerator; otherwise, $\gamma_i^\nu$ denies the strategy by taking the value of 0, which results in the minimum value of the payoff function $\lambda_i^\nu$ (equal to 0).
- $|D^\nu|$: It reflects and minimizes the energy exchange between the prosumer and other utility grids (e.g., main grid) for satisfying a player's expected energy load. This factor is placed in the denominator, so that the lower $|D^\nu|$ is, the higher $\lambda_i^\nu$ is.

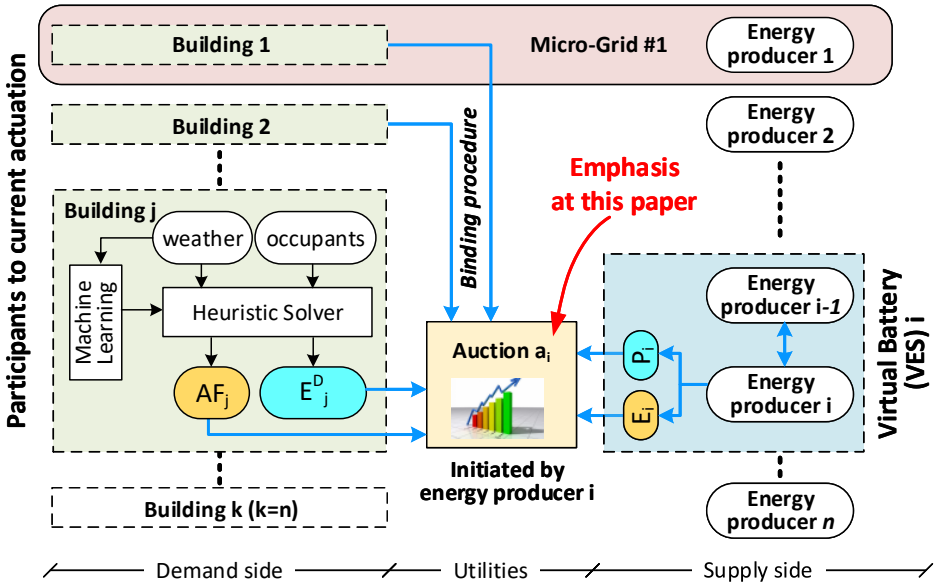


**Figure 4.** The proposed energy trading framework. Expected loads per energy prosumer (left part of the figure) are calculated based on [42].

The studied energy auction problem is solved with a mixed strategy game theory. Instead of the complete definition of players' selections in a pure strategy game, the outcome of mixed strategy games depends not only on a player's own actions, but also on the actions of other players. In order to realize such an auction, a probability is assigned to each pure strategy; thus, each player can randomly selects a pure strategy. More precisely, we consider that player $i$ adopts one pure strategy $s_i^{j_i} \in S_i$ with probability $P_i^{j_i}$. In such a case, the mixed strategy of player $i$ ($P_i$) is defined as

$$P_i^{j_i} | j_i = 1, 2, \ldots, g_i \tag{13}$$

and Equation (14) is applied:

$$\sum_{j_i=1}^{g_i} \left( P_i^{j_i} \right) = 1 \tag{14}$$

The mixed strategy combination regarding all prosumers is expressed as $P = P(P_{-i}, P_i)$, where $P_{-i}$ refers to a set of mixed strategies for all the prosumers except prosumer $i$. Based on this, Equation (15) gives player $i$'s payoff value for a mixed strategy combination $P$, where $s = \{s_1^{j_1}, s_2^{j_2}, \ldots, s_n^{j_n}\}$.

$$\lambda_i(P) = \sum_{s \in S} \left( \lambda_i(S) \times \prod_{i \in N} \left( P_i^{j_i} \right) \right) \tag{15}$$

The previously mentioned game's formulation seeks to compute a Nash equilibrium statement. More specifically, a mixed strategy combination $P^*$ corresponds to a Nash equilibrium if Equation (16) is satisfied, where $V_i$ refers to all the mixed strategies for prosumer $i$. This is equivalent to the optimization problem described by Equation (17) [45]. The $\beta_i$ parameter in this notation refers to an ancillary variable that represents the highest possible payoff for prosumer $i$, while its value is computed by Equation (17).

$$\lambda_i(P^*) \geq \lambda_i\left(P^{*-i}, P^i\right), \forall i \in N \text{ and } \forall P_i \in V_i \tag{16}$$

$$\begin{aligned} \min\left(\sum_{i\in N}\left(\beta_i - \lambda_i(P)\right)\right) \\ s.t. P_i\left(P_{-i}, s_i^{j_i}\right) - \beta_i \leq 0, \forall j_i = 1, 2, \ldots, g_i, \forall i \in N \\ \sum_{j_i=1}^{g_i}\left(P_i^{j_i}\right), \forall i \in N \\ P_i^{i_j} \geq 0, \forall i_j = 1, 2, \ldots, g_i, \forall i \in N \end{aligned} \tag{17}$$

Considering that player $i$'s payoff value in the strategy combination $P$ is $\lambda_i(P)$, the objective function of the optimization problem (as described by Equation (17)) is to minimize the sum of differences between the payoff value $\lambda_i(P)$ in the strategy combination $P$ and the highest possible payoff value $\beta_i$, in order that after the optimization, the calculated strategy combination $P$ corresponds to the highest possible payoff value for all the participants. Detailed proof that this strategy combination $P$ corresponds to a Nash equilibrium of the game studied is provided in [45].

The time complexity for computing the Nash equilibrium for an $N \times K$-player game with $g_i = 4$ strategies per player is given by $O(N \times K \times 4^{N\times K})$ [46]. In order to overcome the complexity challenge and favor faster converge to equilibrium, different optimizations are applied to prune the search space by eliminating players' selections that lead apriori to non-optimal solutions (e.g., discard strategies that lead to non-optimal energy flows in micro-grid-to-grid and VES-to-micro-grid integrations, as they are computed based on the $Q$ threshold [6]). Further run-time enhancement is feasible with the proposed hardware/software co-design on the target low-cost FPGA platform. The experimental results in Section 5 highlight the efficiency of these selections.

### *4.2. Algorithm for Computing Equilibrium*

Algorithm 1 gives the proposed pseudo-code for solving the energy trading problem. In the initialization phase, energy producer $i$ sets its total energy for selling $(E_i^M)$, as well as the minimum energy that can be traded in the market $(E_i^P)$. Then, a number of $H_i$ simultaneous auctions are instantiated in parallel, where $E_i^M = H_i \times E_i^P$. Consumers express their interest in participating in these auctions. However, in order for this interest to be acceptable, their associated VES needs to have enough capacity to store the currently traded energy (in case a consumer wins all the auctions in which they participate). Equation (18) formulates this constraint in order for consumer $i$ to participate in an auction.

$$\sum_{\forall\ auctions}\left(E_i^M\right) \leq E_i^{B,max} - E_i^B \tag{18}$$

Also, during the initialization phase, the participants set their minimum $(M_i^{min})$ and maximum $(M_i^{max})$ reservation prices at which they are willing to continue energy trading. These reservation prices are confidential, and their values might differ among prosumers. In detail, the reservation price for consumer $i$ depends on their available funds, the expected energy loads, and their energy generation forecast. Similarly, reservation prices for producer $i$ depend on the VES charge level $E_i^B$, as it defines the maximum possible energy storage. Variations in prosumers' reservation prices result in different aggressiveness for buying/selling the traded energy, which in turn allows different forms of dynamic pricing policies for multiple markets and customers depending on the consumers' willingness to pay based on the demand and response curve.

**Algorithm 1:** Pseudo-code for solving auction $a_i$.

```
Input: number of players N
Input: max energy budget E_i^M from prosumer i
Function Find Equilibrium
calculate partial budget E_i^P ≤ E_i^M per sub-game
foreach partial sub-game ∈ H_i do
    compute M_i^min, M_i^max per E_i^P and energy source
    while not reach R do
        foreach player do
            calculate Q based on [6]
            find validstrategies based on Q ≥ 75%
            foreach valid strategy ∈ S do
                update bids based on Equation (19)
                compute payoffs (λ) based on Equation (12)
                check_equilibrium(equilibrium)
            end
        end
        update F_i(r)
        T_i++
    end
end
Function check_equilibrium(equilibrium)
if (equilibrium = Nash) then
    accept energy import/export
    update AF based on Equation (9)
end
if (equilibrium != Nash) then
    if (λ ≥ optimum_payoff) then
        update optimum_solution
        update optimum_payoff
    end
end
```

Equation (19) gives player $i$'s unit price, or bid, $B_i(r)$ at round $r$, where $B_i(r-1)$ denotes the player's previous bid, $T_i$ is the number of consecutive rounds until consumer $i$ wins an auction (it refers to the total number of rounds if a consumer participates in more than one auction simultaneously), $F_i(r)$ is the bidding aggressiveness, and $\Delta B_i(r)$ expresses the sensitivity to price, which denotes the degree to which the current energy price affects consumers' purchasing behaviors. The computed $B_i(r)$ values are confidential among consumers (only the energy producer that initiates the game is aware of them) and their value respects consumer $i$'s maximum reservation price ($B_i^{max}$). Similar to the reservation price, bidding aggressiveness is also related to the elasticity of demand, which considers that in case all other market factors remain constant, a relative price increase leads to a drop in the quantity demanded. High elasticity corresponds to a case where consumers are more willing to buy energy budgets even after price increases. On the other hand, under inelastic demand even small price increases may significantly lower demand. Additional discussion on the $F_i(r)$ parameter is given at the end of this section.

$$B_i(r) = B_i(r-1) + \frac{T_i \times \Delta B_i(r)}{F_i(R)} \tag{19}$$

The equilibrium statement, as well as its efficiency, is affected by the maximum number of game rounds ($R$). More precisely, the participants in the studied game are aware that the auction is being "played" a specific (finite) number of rounds, and that the game ends for certain (if there is no equilibrium) after $R$ rounds have been played. As we proceed to the

maximum number of game rounds $R$, the bids increase, so that the probability of a match in the next round is elevated. In case there is no equilibrium after $R$ rounds, consumers import the requested energy from the main grid at the regulator's flat rate ($D^{imp}$), while the energy producer exports the traded energy $E_i^P$ to the main grid at the regulator's feed-in tariff ($D^{exp}$). In any case, the minimum bid in auctions is higher than the corresponding cost that an electricity utility has to pay to a private, independent energy producer in the grid ($M_i^{min} \geq D^{exp}$). Similarly, the maximum bid is lower than the corresponding energy cost from the main grid ($M_i^{max} \leq D^{imp}$). Consequently, both consumers and producers favor energy transactions through the proposed electricity market, as it maximizes their profit $AF$.

### *4.3. Framework Customization for Energy Trading*

Up to now, we have discussed a general-purpose orchestrator in order to decide upon prosumers' selections in a cyber–physical system. In this subsection, we customize a number of framework parameters in order to maximize the efficiency of the proposed energy trading mechanism.

The converge to equilibrium in our game-theory approach is affected by consumer $i$'s bidding aggressiveness $F_i(r)$ [34]. Instead of setting a static value for this parameter, the proposed framework defines the value of $F_i(r)$ as a function of the current game's round $r$, where $0 \leqslant r \leqslant R$. For the scope of this manuscript, five representative aggressiveness schemes (depicted in Figure 5) are evaluated, where the initial $(F_i(0))$ and final bidding aggressiveness $(F_i(R))$ are identical among them. Table 4 summarizes the results from this analysis in term of average $AF$ improvement over the initially assigned funds, as computed by Equation (21) for the 52-week experiment. Based on this analysis, the optimal strategy for updating consumer's aggressiveness is the one depicted in Figure 5a, since it improves the $AF$ metric on average by 16%. Hence, for the rest of our experimentation, the $F_i(r)$ parameter is defined according to Equation (20).

$$F_i(r) = F_i(0) \times e^{-\left(\left(\frac{1}{R^2}\right) \times \left(\ln \frac{F_i(0)}{F_i(R)}\right) \times r\right)} \tag{20}$$

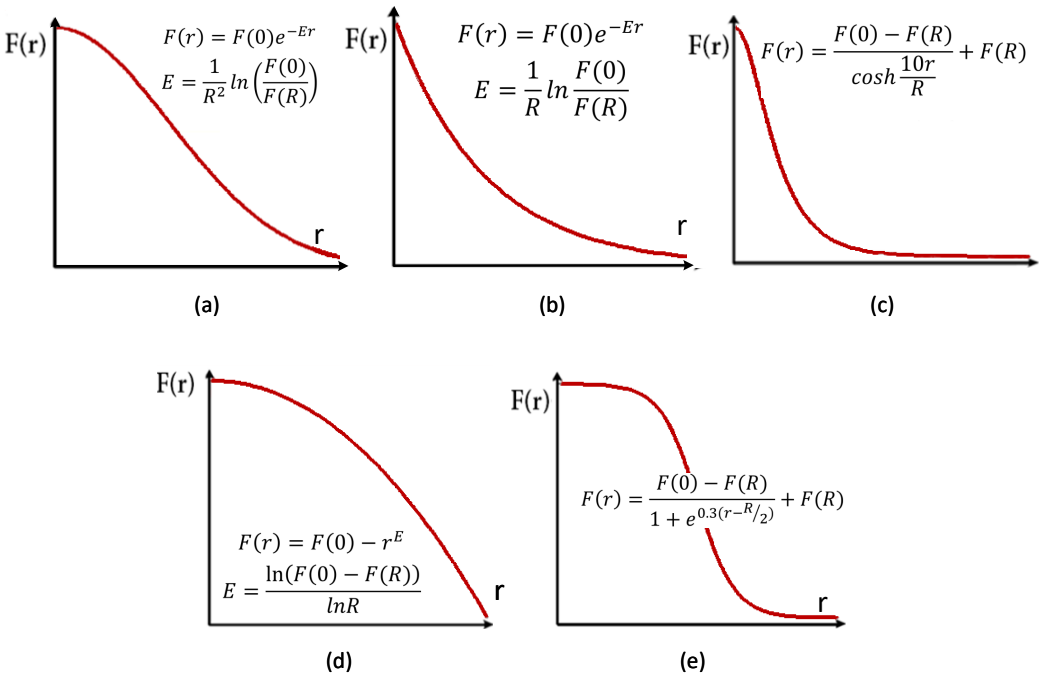


**Figure 5.** Candidate bidding aggressiveness schemes.

**Table 4.** Evaluating consumer bidding aggressiveness.

| Bidding Aggressiveness | Average Profit Based on Equation (21) |
|---|---|
| Figure 5a | 16% |
| Figure 5b | 2% |
| Figure 5c | 7% |
| Figure 5d | 9% |
| Figure 5e | −18% |

The chronology of players' selections during an auction is also of high importance for solvers that rely on game theory. Two representative chronologies, namely, sequential and simultaneous, are studied and evaluated throughout this manuscript. In sequential auctions, bidders move in turns and eventually reach an equilibrium. In contrast, in simultaneous auctions (also known as "one-shot") players cannot react to their opponents, since their actions are chosen simultaneously. The chronology also affects the way that players' selections are evaluated. Specifically, whereas the utility function can be evaluated after each round in simultaneous auctions, it is evaluated only once at the end of a sequential auction.

In order to study this parameter in detail, both chronologies are quantified in terms of improving the $AF$ metric and the results are plotted in Figure 6. For demonstration purposes, the values on the vertical axis are given in a normalized manner over the initial funds assigned per micro-grid ($AF^{init}$) based on Equation (21). These values refer to the average (among 100 micro-grids) variation in available funds during the 1-year experiment. According to this figure, both chronologies improve prosumers' $AF$ metrics over the reference solution, while this improvement is even higher for sequential auctions. Such a superiority is mainly due to the players' flexibility to react to the opponents selections; however, for the rest of our analysis, only the simultaneous auction mechanism will be explored, as it better respects the energy market's specification for simultaneous bidding without knowledge about the strategies adopted by other players.

$$plotted\ value = \sum_{i=1}^{100}\left(\frac{AF_i}{AF_i^{init}}\right) \times 100\% \tag{21}$$

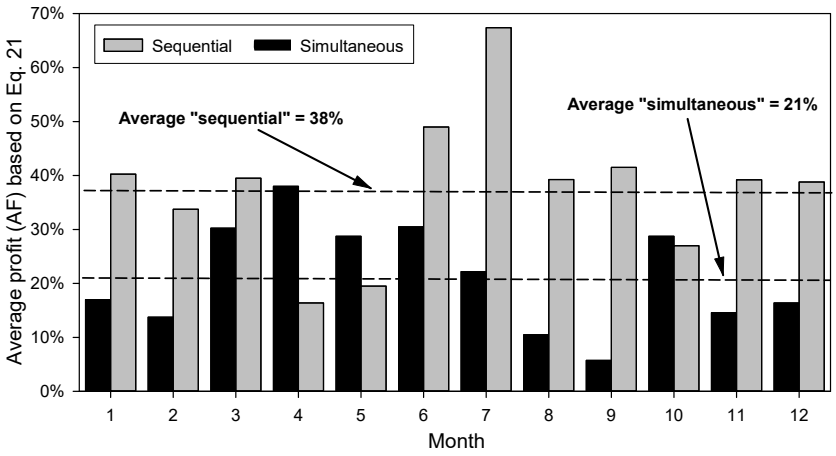


**Figure 6.** Performance of simultaneous and sequential auctions.

## 5. Evaluation Analysis

The efficiency of the proposed framework is quantified with a distributed auction scenario consisting of 100 energy prosumers that follow the template depicted in Table 3. The expected energy loads $E_i^D$, the electricity generation $E_i^{RS}$ forecast, as well as the variation in available funds $AF_i$ per prosumer are computed according to the approach discussed

in Section 3. For this purpose, publicly available data for weather [39] and the regulator's energy prices [38] are employed for the 52-week experiment. Also, an initial amount of funds ($AF_i^{init}$) is assigned per prosumer, as formulated by Equation (4).

By allowing micro-grids to trade and define the price per kWh on a dynamical basis, the proposed framework aims to reduce the overall energy cost and maximize the prosumers' profit. The rest of this section quantifies the efficiency of the introduced framework to compute optimal bids that result in equilibrium statement. For evaluation purposes, the corresponding results retrieved with two well-established MPC solvers, namely, Pattern Search [47] and Fmincon [48], are also provided. It is worth highlighting that instead of existing CPS orchestrators that impose excessive complexity, the results that affect the introduced auction framework are retrieved with a low-cost embedded device.

The proposed auction framework enables consumers to participate in multiple auctions simultaneously in order to bid in a more conservative way, and hence maximize their $AF$ metric. For the scope of this analysis, we consider that an energy producer $i$ instantiates up to $H_i = 50$ partial sub-games (auctions), where up to 100 consumers are involved in each of them (assuming that they respect the constraint defined by Equation (18)). The value of $H_i$ is dynamically defined, since each energy producer decides the energy budget to be exported ($E_i^M$) on demand, as well as the minimum energy that can be traded in the market ($E_i^P$). The participant consumers place their bids according to Equation (19) based on their own strategy and aggressiveness.

The impact of this parameter is explored in Figure 7, where auctions with one and multiple sub-games are evaluated. The vertical and horizontal axes of this figure give the average energy cost per kWh among the 100 micro-grids and the maximum number of participants per auction, respectively. For demonstration purposes, these values are plotted in a normalized manner over the main grid's flat rate ($D^{imp}$). Based on Figure 7, consumers achieve significant savings when they participate in multiple auctions simultaneously. Specifically, our exploration indicates that the proposed framework leads to average energy cost savings per kWh for single and multiple partial auctions of 15% and 26%, respectively, as compared to main grid's flat rate. Consequently, for the rest of our analysis we consider that consumers trade energy prices with multiple (at least one) producers, each of which initiates up to $H_i = 50$ partial sub-games in parallel.

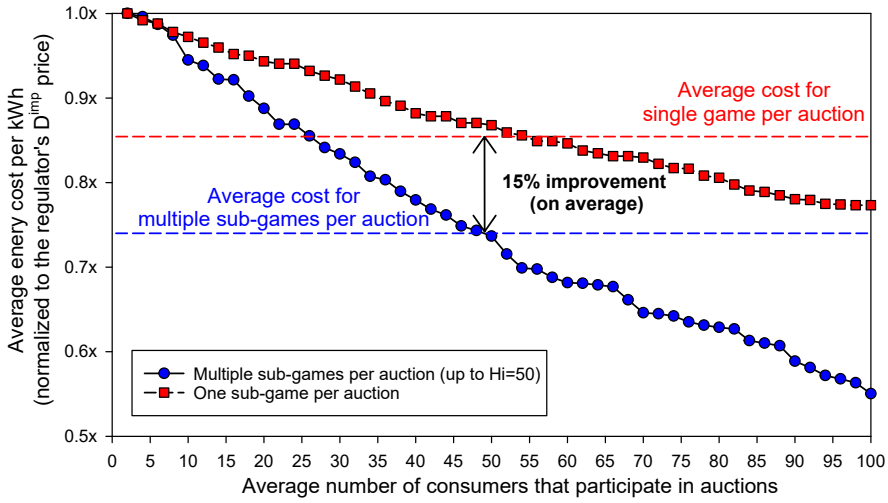


**Figure 7.** Efficiency of multiple partial auctions.

Next, we evaluate the efficiency of the proposed framework in improving the $AF$ metric by enabling prosumers to share energy. For this purpose, we explore the impact of VES cluster size, where different number of neighboring prosumers are assigned to a common VES. Specifically, we consider clusters that group from 2 up to 10 energy prosumers per VES, where participants are randomly selected from the five templates

depicted in Table 3. In order to avoid the impact of random micro-grid clustering, this experiment was repeated 20 times and the results are summarized in Figure 8. Three different curves are plotted in this figure, which correspond to worst-case, best-case, and median solutions among the reported results. The vertical axis of this diagram denotes, in a normalized manner, the average increase in the prosumers' profit among the studied 100 micro-grids over the reference solution without considering VES clustering. Note that the valid solutions that are evaluated in this figure respect the threshold $Q \geq 75\%$ of the proposed auction framework (Algorithm 1).

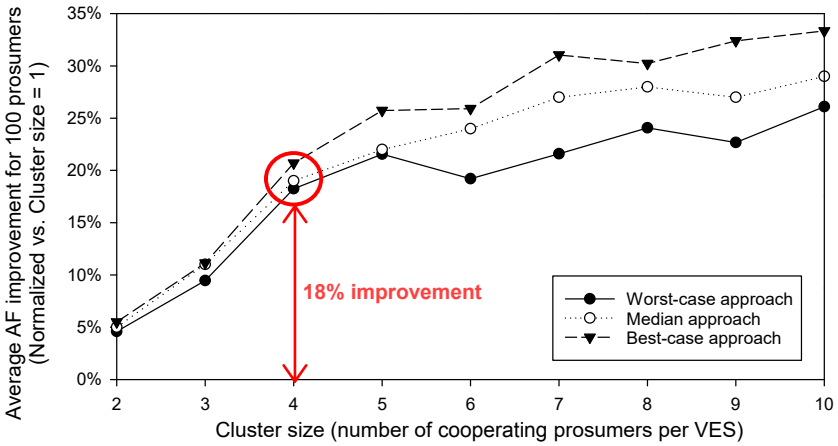


**Figure 8.** Impact of cluster size on the auction's outcome.

The results from this analysis indicate that larger clusters improve the overall profit of the prosumers because consumers bid in a more conservative way. Additionally, larger clusters enable more advanced strategies to be applied among consumers (e.g., benefit from increased VES capacity to hedge against energy generation uncertainty). However, such an efficiency seems to be saturated for clusters with more than four prosumers. Although this conclusion depends on the VES capacity, as well as the prosumers' expected loads and their energy generation forecasts, the additional $AF$ improvement for clusters with more partners is negligible as compared to the excessive increase in computational complexity for finding the Nash equilibrium. Thus, the rest of our experimentation considers a VES cluster size equal to 4.

Apart from the cluster size, the VES capacity is also of high importance, since it defines the maximum energy storage per cluster of cooperative prosumers. In order to study this parameter in detail, we consider VES capacities that range from 10% (initial configuration discussed in Equation (3)) up to 25% of the buildings' average daily expected energy loads. Similar to the previous experiments, three scenarios are evaluated during this analysis, namely, the worst-case, best-case, and median-case among the 20 executions, and the results are summarized in Table 5. According to this analysis, the energy sharing between prosumers leads to significant improvement in their profit $AF$. Although one might expect that the increase in the VES's capacity results in a monotonic increase in the $AF$ parameter, this is not always the case, because the VES capacity enables more advanced strategies for energy prosumers (i.e., charge the VES with part of the energy from renewable sources). The results summarized in this table also evaluate the efficiency of the proposed solution (median case) against the Pattern Search and Fmincon MPC solvers. More specifically, the introduced framework exhibits comparable performance to well-established solvers, but with significantly lower computational complexity (as we discuss more thoroughly in Section 5.1). Consequently, for the rest of our experimentation we consider that the VES capacity is 10% of the average daily expected energy loads of consumers, as defined by Equation (3).

**Table 5.** Impact of VES capacity on *AF* metric (results normalized to the solution without VES sharing).

| **Average Profit Based on Equation (21)** | | **VES Capacity** | | | | |
|---|---|---|---|---|---|---|
| | | **5%** | **10%** | **15%** | **20%** | **25%** |
| Proposed (worst case) | | 4% | 16% | 25% | 33% | 41% |
| Proposed (median case) | | 6% | 23% | 34% | 38% | 45% |
| Proposed (best case) | | 9% | 28% | 37% | 48% | 49% |
| Pattern Search [47] | | 7% | 24% | 34% | 41% | 47% |
| Fmincon [48] | | 9% | 29% | 39% | 45% | 51% |
| Proposed (median) | vs. Pattern Search | 16.6% | 4.3% | 0.0% | 7.9% | 4.4% |
| | vs. Fmincon | 50% | 26.1% | 14.7% | 18.4% | 13.3% |

In order to study the efficiency of this selection in detail, Figure 9 visualizes, with different colors, the average charge status for the studied VES capacity per energy prosumer (horizontal axis) and experiment week (vertical axis). Since our system relies on clusters of prosumers that share a common VES, all of them are marked with the same color. According to this analysis, the average VES charge during the 52-week experiment is 72%, while the charge of the VES systems for all the prosumers is at least 40%.

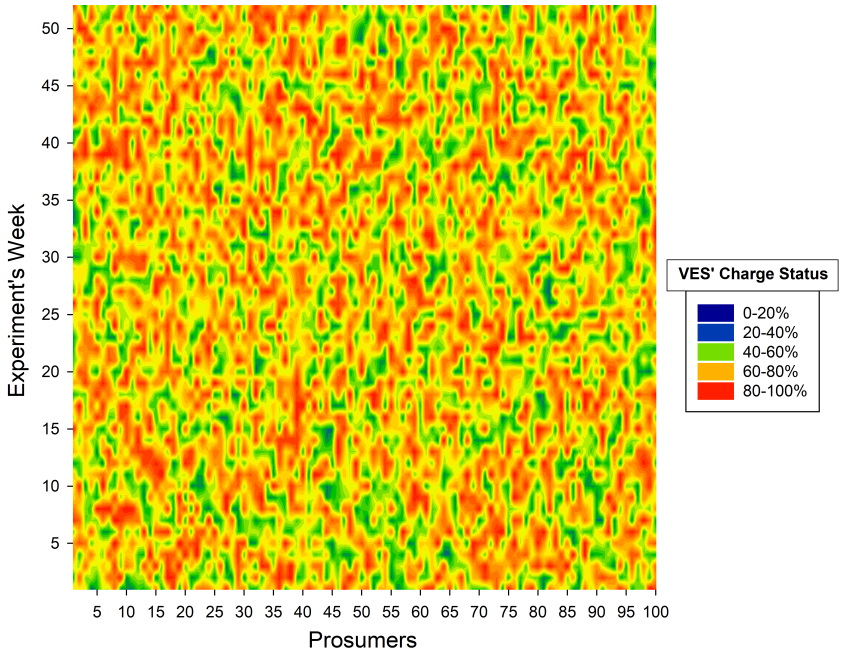


**Figure 9.** VES charge during the 52-week experiment.

As we have already mentioned, the improvement in the *AF* metric, and hence the reduction in energy cost per kWh, also depends on the maximum number of rounds per auction ($R$). An increased number of rounds favors energy consumers bidding in a more conservative way. Similarly, energy producers decrease their expected profit when moving towards the game's end. By contrast, auctions with fewer rounds force buyers to exhibit a more aggressive strategy in order to reserve the energy from the proposed electricity market rather than from the main grid. The impact of this parameter is further explored in Figure 10, where the average energy cost per kWh among auctions is plotted for auctions with different maximum numbers of rounds ($R$). For demonstration purposes, the values on the vertical axis are normalized over the average energy cost for auctions with $R = 20$. Similar to previous cases, the impact of the random initialization phase is alleviated by performing this experiment 20 times and the reported values correspond to the worst-case, best-case, and median-case results among these executions. According to this figure, the proposed framework leads to an almost constant average energy cost per kWh for auctions consisting of more than 80 rounds. Further experimentation with different clusters

confirms this claim, since such a saturation is almost insensitive either to both the number of players and the prosumers' energy generation and consumption forecasts; it is only related to the players' bidding aggressiveness. Consequently, by taking into account that the number of rounds highly affects the problem's computational complexity, for the rest of the manuscript we consider that $R = 80$. Such a selection reduces the initial energy cost by 62%, on average, which is comparable to the performance of the reference solutions. Specifically, the Pattern Search [47] and Fmincon solvers [48] achieve average savings of 57% and 74%, respectively.

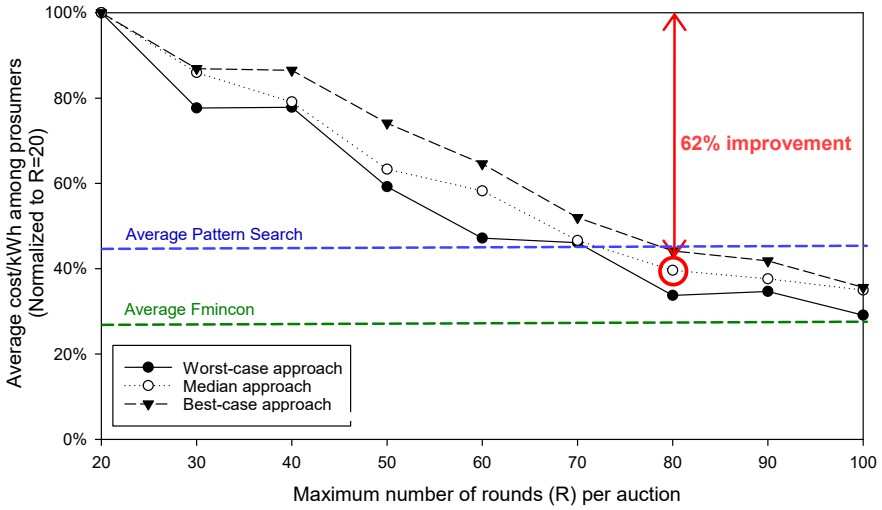


**Figure 10.** Exploration of maximum number of rounds $(R)$ per auction.

### *5.1. Hardware Implementation*

This subsection discusses the hardware implementation of the proposed framework into a low-cost embedded device. For this purpose, the Xilinx Zybo-Z7 ARM/FPGA SoC development board was selected with an 667 MHz dual-core Cortex-A9 processor and 1 GB DDR3 memory. Regarding the physical design, it was performed with the Xilinx Vivado High-Level Synthesis (HLS) suite [49]. For demonstration purposes, a scenario with eight energy producers (FPGA boards) interconnected with a TCP/IP protocol, as depicted in Figure 11, is evaluated. Each of these boards instantiates up to $H_i = 50$ partial sub-games simultaneously (parallel auctions) with up to 100 energy consumers.

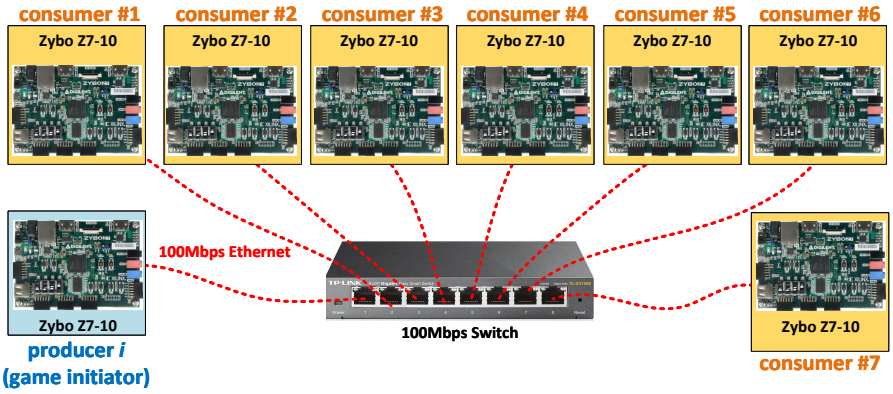


**Figure 11.** Demonstration setup for the proposed distributed auction framework.

The maximization of prosumers' profit is the main objective for the introduced solution. In order to evaluate this parameter, Figure 12 compares the efficiency of three flavors of the proposed framework. More precisely, the first approach (reference solution) considers that prosumers import/export energy only from/to the main grid at $D^{imp}$ and

$D^{exp}$ rates. On the other hand, the second and third approaches rely on the day-ahead and the week-ahead markets, where auctions are performed 1 day and 1 week in advance of the energy delivery, respectively. Note that this analysis refers to the overall evaluation of the proposed framework, since it takes into account already-derived conclusions about weather forecast, expected loads and energy generation forecasts, consumers' aggressiveness (Table 4), simultaneous auctions (Figure 6), multiple sub-games per auction (Figure 7), cluster size (Figure 8), VES capacity (Table 5), and the maximum number of rounds per auction (Figure 10).

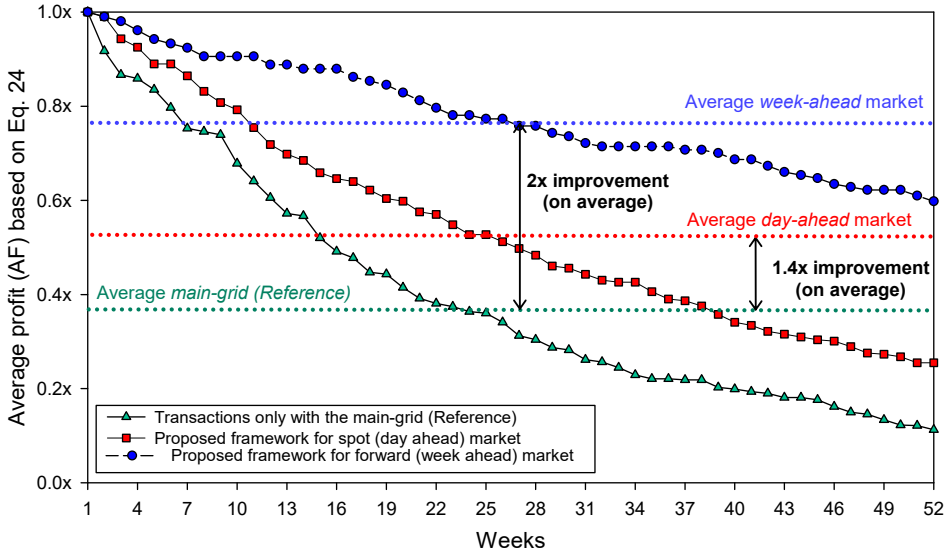


**Figure 12.** Efficiency for energy transactions that are performed (i) at run-time, (ii) a week ahead, and (iii) a day ahead.

Since energy prosumers import/export energy from/to the main grid at higher/lower prices compared to the proposed electricity market, this leads to lower $AF$ values, as highlighted by the reference solution in Figure 12. On the other hand, the proposed framework achieves average energy savings for the spot (day-ahead) and forward (week-ahead) markets of 1.4× and 2×, respectively. Such a superiority is mainly due to the optimal selection of prosumer's strategies, which efficiently utilize the VES system in order to hedge against energy generation uncertainty and price fluctuations. This figure is also annotated with the corresponding results from the Fmincon and Pattern Search MPC solvers, which achieve average $AF$ improvements of 1.5× and 1.2×, respectively. However, such improvements impose notable computational overhead, which cannot be tackled using low-cost processing cores.

In order to discuss this aspect more thoroughly, we also explore the run-time overhead for computing the equilibrium statement. Towards this, Figure 13 plots the variation in the maximum operation frequency (vertical axis) for different numbers of simultaneous games (horizontal axis), each of which has the maximum number of partial sub-games ($H_i = 50$). This analysis indicates that even for the border case, the proposed hardware implementation exhibits a performance degradation of about 27% due to the additional signaling overhead among players. However, even in this case, the equilibrium is computed at less than a second (on average at 0.87 s). On the other hand, the state-of-the-art MPC solvers, such as the Pattern Search and Fmincon algorithms, impose considerable run-time overhead, since they compute optimal bids by exhaustively exploring the design space. Specifically, the solutions for the Pattern Search and Fmincon solvers were retrieved after 2.5 h on a 4-core Intel(R) i5-6500 CPU@3.20 GHz with 32 GB RAM. Consequently, we conclude that the proposed hardware prototype achieves on average a speedup of 4 orders of magnitude. Finally, it is worth noting that the available resources of the employed low-cost FPGA platform (Zybo-Z7) are enough to realize up to $H_i$ = 240 games in parallel.

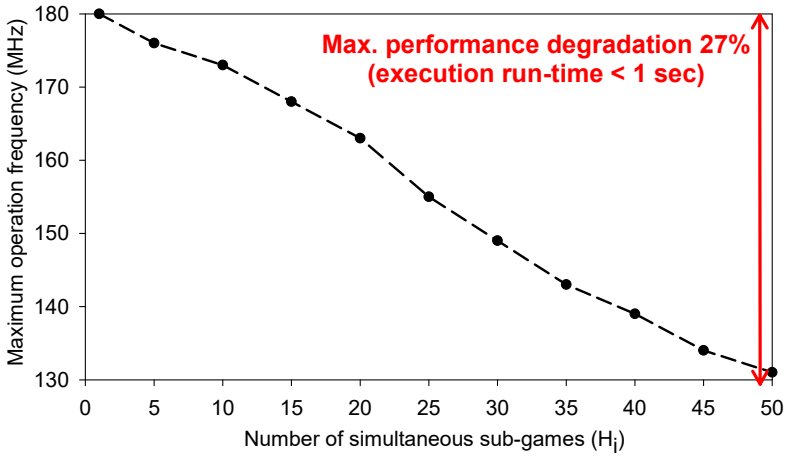


**Figure 13.** Execution run-times for different numbers of simultaneous games $(H_i)$ per auction $a_i$.

### *5.2. Social Impact*

Specifically, the facilitation of local energy generation and trading fosters the development of decentralized energy networks, mitigating vulnerabilities associated with centralized grid dependencies and enhancing community resilience in the face of unforeseen disruptions. Furthermore, by empowering small-scale producers, the framework promotes energy independence and security, reducing reliance on external sources and mitigating risks associated with price volatility and supply chain disruptions.

From an environmental standpoint, the platform incentivizes the integration of renewable energy sources, accelerating the transition towards sustainable energy systems and contributing to the mitigation of greenhouse gas emissions. Additionally, the intelligent decision-making capabilities embedded within the framework enable optimized energy utilization within the micro-grid, minimizing waste and promoting responsible consumption patterns.

Beyond resilience and sustainability, the framework has profound socio-economic implications. By enabling active participation in energy markets, the platform generates new income streams for small-scale producers, stimulating local economic development and fostering self-sufficiency. Moreover, the platform cultivates a sense of shared responsibility and collective ownership of energy resources within communities, encouraging collaborative efforts towards sustainable energy management and enhancing social cohesion.

## 6. Conclusions and Future Directions

A novel framework for orchestrating cyber–physical systems based on game theory was introduced. The proposed solution was applied in order to decide optimal bidding in distributed energy auctions among micro-grids. Experimental results based on real data validate the efficiency of the proposed solution, since it achieves average energy cost savings up to 2×, as compared to the corresponding main grid's flat rate. Moreover, the proposed orchestrator achieves comparable (or superior) performance compared to relevant online and MPC controllers. Apart from economic benefits, such a result also has a social impact, as it enables small-scale energy producers to become active players in the energy market. Finally, we show that the hardware implementation of the proposed framework on a low-cost embedded device exhibits similar performance to relevant state-of-the-art MPC solvers but with significantly lower computational complexity.

Future investigations could also examine the integration of blockchain technology, which presents a compelling suite of functionalities poised to augment distributed energy transaction frameworks. Its immutable ledger ensures transparency and accountability by providing an unalterable record of all energy transactions, mitigating the risk of fraudulent activities. In addition to that, cryptographic mechanisms inherent in blockchain technology safeguard sensitive data and bolster system integrity by securing energy transactions.

Furthermore, the utilization of smart contracts automates and streamlines transaction processes, thereby enhancing market efficiency and reducing administrative overhead. Apart from that, blockchain technology provides a decentralized architecture conducive to P2P energy trading, empowering prosumers and promoting community-based energy solutions. In essence, blockchain technology can serve as a catalyst for the transition towards decentralized, secure, and efficient energy systems, empowering communities and individuals to actively participate in the evolving energy landscape.

Finally, we have to mention that while cost effectiveness is crucial for wider adoption, it is essential to consider the potential limitations of low-cost FPGA devices in demanding real-time applications. In detail, aspects like device reliability are primarily influenced by fabrication and operational factors: cost can indirectly impact these aspects. To mitigate potential concerns, our future work will focus on incorporating redundancy mechanisms, employing robust design practices, and conducting extensive real-world testing. Furthermore, we will investigate the long-term reliability of these devices and explore strategies for scaling the framework to accommodate larger micro-grid networks.

**Funding:** This research received no external funding.

**Informed Consent Statement:** Not applicable.

**Data Availability Statement:** The original data presented in the study are openly available in [38,39].

**Conflicts of Interest:** The author declares no conflicts of interest.

## References

1. Palensky, P.; Dietrich, D. Demand Side Management: Demand Response, Intelligent Energy Systems, and Smart Loads. *IEEE Trans. Ind. Inform.* **2011**, *7*, 381–388. [CrossRef]
2. Lavrijssen, S.; Carrillo Parra, A. Radical Prosumer Innovations in the Electricity Sector and the Impact on Prosumer Regulation. *Sustainability* **2017**, *9*, 1207. [CrossRef]
3. Diamantoulakis, P.D.; Kapinas, V.M.; Karagiannidis, G.K. Big Data Analytics fo Dynamic Energy Management in Smrart Grids. *Big Data Res.* **2015**, *2*, 94–101. [CrossRef]
4. Morstyn, T.; Teytelboym, A.; Mcculloch, M.D. Bilateral Contract Networks for Peer-to-Peer Energy Trading. *IEEE Trans. Smart Grid* **2019**, *10*, 2026–2035. [CrossRef]
5. Zhang, C.; Wu, J.; Long, C.; Cheng, M. Review of Existing Peer-to-Peer Energy Trading Projects. *Energy Procedia* **2017**, *105*, 2563–2568. [CrossRef]
6. Sadamoto, T.; Chakrabortty, A.; Ishizaki, T.; ichi Imura, J. Dynamic Modeling, Stability, and Control of Power Systems with Distributed Energy Resources. *IEEE Control. Syst. Mag.* **2018**, *39*. 34–65. [CrossRef]
7. Xilinx. Zybo Z7-10: Zynq-7000 ARM/FPGA SoC Development Board. 2018. Available online: https://www.xilinx.com/products/boards-and-kits/1-pukimv.html (accessed on 2 November 2024).
8. Dutta, G.; Mitra, K. A literature review on dynamic pricing of electricity. *J. Oper. Res. Soc.* **2017**, *68*, 1131–1145. [CrossRef]
9. Siozios, K.; Anagnostos, D.; Soudris, D.; Kosmatopoulos, E. *IoT for Smart Grids: Design Challenges and Paradigms*; Springer International Publishing: Cham, Switzerland, 2019; p. 282. [CrossRef]
10. Wan, C.; Zhao, J.; Song, Y.; Xu, Z.; Lin, J.; Hu, Z. Photovoltaic and solar power forecasting for smart grid energy management. *CSEE J. Power Energy Syst.* **2015**, *1*, 38–46. [CrossRef]
11. Ren, H.; Wu, Q.; Gao, W.; Zhou, W. Optimal operation of a grid-connected hybrid PV/fuel cell/battery energy system for residential applications. *Energy* **2016**, *113*, 702–712. [CrossRef]
12. Morales, J.M.; Conejo, A.J.; PÉrez-Ruiz, J. Short-Term Trading for a Wind Power Producer. *IEEE Trans. Power Syst.* **2010**, *25*, 554–564. [CrossRef]
13. Liu, N.; Yu, X.; Wang, C.; Li, C.; Ma, L.; Lei, J. Energy-Sharing Model with Price-Based Demand Response for Microgrids of Peer-to-Peer Prosumers. *IEEE Trans. Power Syst.* **2017**, *32*, 3569–3583. [CrossRef]
14. Motalleb, M.; Ghorbani, R. Non-cooperative game-theoretic model of demand response aggregator competition for selling stored energy in storage devices. *Appl. Energy* **2017**, *202*, 581–596. [CrossRef]
15. Wang, Y.; Saad, W.; Han, Z.; Poor, H.V.; Basar, T. A Game-Theoretic Approach to Energy Trading in the Smart Grid. *IEEE Trans. Smart Grid* **2014**, *5*, 1439–1450. [CrossRef]
16. Molina, J.; Zolezzi, J.; Contreras, J.; Rudnick, H.; Reveco, M. Nash-Cournot Equilibria in Hydrothermal Electricity Markets. *IEEE Trans. Power Syst.* **2011**, *3*, 1089–1101. [CrossRef]
17. Zhang, C.; Wu, J.; Zhou, Y.; Cheng, M.; Long, C. Peer-to-Peer energy trading in a Microgrid. *Appl. Energy* **2018**, *220*, 1–12. [CrossRef]

18. Liu, T.; Tan, X.; Sun, B.; Wu, Y.; Guan, X.; Tsang, D.H.K. Energy management of cooperative microgrids with P2P energy sharing in distribution networks. In Proceedings of the 2015 IEEE International Conference on Smart Grid Communications (SmartGridComm), Miami, FL, USA, 2–5 November 2015; pp. 410–415. [CrossRef]
19. Gregoratti, D.; Matamoros, J. Distributed Energy Trading: The Multiple-Microgrid Case. *IEEE Trans. Ind. Electron.* **2015**, *62*, 2551–2559. [CrossRef]
20. Mohamed, F.A.; Koivo, H.N. Online Management of MicroGrid with Battery Storage Using Multiobjective Optimization. In Proceedings of the 2007 International Conference on Power Engineering, Energy and Electrical Drives, Setubal, Portugal, 12–14 April 2007; pp. 231–236. [CrossRef]
21. Clarke, J.; Conner, S.; Fujii, G.; Geros, V.; Jóhannesson, G.; Johnstone, C.; Karatasou, S.; Kim, J.; Santamouris, M.; Strachan, P. The role of simulation in support of Internet-based energy services. *Energy Build.* **2004**, *36*, 837–846. [CrossRef]
22. Magni, L.; De Nicolao, G.; Magnani, L.; Scattolini, R. A stabilizing model-based predictive control algorithm for nonlinear systems. *Automatica* **2001**, *37*, 1351–1362. [CrossRef]
23. Mayne, D.Q.; Rawlings, J.B.; Rao, C.V.; Scokaert, P.O. Constrained model predictive control: Stability and optimality. *Automatica* **2000**, *36*, 789–814. [CrossRef]
24. Carrion, M.; Philpott, A.B.; Conejo, A.J.; Arroyo, J.M. A Stochastic Programming Approach to Electric Energy Procurement for Large Consumers. *IEEE Trans. Power Syst.* **2007**, *22*, 744–754. [CrossRef]
25. Khatib, T.; Mohamed, A.; Sopian, K. Optimization of a PV/wind micro-grid for rural housing electrification using a hybrid iterative/genetic algorithm: Case study of Kuala Terengganu, Malaysia. *Energy Build.* **2012**, *47*, 321–331. [CrossRef]
26. Parisio, A.; Rikos, E.; Tzamalis, G.; Glielmo, L. Use of model predictive control for experimental microgrid optimization. *Appl. Energy* **2014**, *115*, 37–46. [CrossRef]
27. Parisio, A.; Rikos, E.; Glielmo, L. A Model Predictive Control Approach to Microgrid Operation Optimization. *IEEE Trans. Control Syst. Technol.* **2014**, *22*, 1813–1827. [CrossRef]
28. Chaouachi, A.; Kamel, R.M.; Andoulsi, R.; Nagasaka, K. Multiobjective Intelligent Energy Management for a Microgrid. *IEEE Trans. Ind. Electron.* **2013**, *60*, 1688–1699. [CrossRef]
29. Tutkun, N. Minimization of operational cost for an off-grid renewable hybrid system to generate electricity in residential buildings through the SVM and the BCGA methods. *Energy Build.* **2014**, *76*, 470–475. [CrossRef]
30. Kyriakarakos, G.; Dounis, A.I.; Arvanitis, K.G.; Papadakis, G. A fuzzy logic energy management system for polygeneration microgrids. *Renew. Energy* **2012**, *41*, 315–327. [CrossRef]
31. Chao, H.P.; Butler Wilson, R. Multi-dimensional Procurement Auctions for Power Reserves: Robust Incentive-Compatible Scoring and Settlement Rules. *J. Regul. Econ.* **2002**, *22*, 161–183. [CrossRef]
32. Danassis, P.; Siozios, K.; Korkas, C.; Soudris, D.; Kosmatopoulos, E. A low-complexity control mechanism targeting smart thermostats. *Energy Build.* **2017**, *139*, 340–350. [CrossRef]
33. Velik, R.; Nicolay, P. Grid-price-dependent energy management in microgrids using a modified simulated annealing triple-optimizer. *Appl. Energy* **2014**, *130*, 384–395. [CrossRef]
34. Wang, X.; Zhang, Y.; Zhang, S.; Li, X.; Wu, L. Equilibrium Analysis of Electricity Markets With Microgrids Based on Distributed Algorithm. *IEEE Access* **2019**, *7*, 119823–119834. [CrossRef]
35. Folgado, F.J.; Calderón, D.; González, I.; Calderón, A.J. Review of Industry 4.0 from the Perspective of Automation and Supervision Systems: Definitions, Architectures and Recent Trends. *Electronics* **2024**, *13*, 782. [CrossRef]
36. Hasan, M.K.; Abdulkadir, R.A.; Islam, S.; Gadekallu, T.R.; Safie, N. A review on machine learning techniques for secured cyber-physical systems in smart grid networks. *Energy Rep.* **2024**, *11*, 1268–1290. [CrossRef]
37. Department of Energy, U.S. EnergyPlus Energy Simulation Software. 2015. Available online: https://www.energy.gov/eere/buildings/articles/energyplus (accessed on 2 November 2024).
38. Energy_Market_Operator. Public Energy Price Data. 2018. Available online: https://www.aemo.com.au/Electricity/National-Electricity-Market-NEM (accessed on 4 May 2018).
39. Weather. Public Weather Data. 2018. Available online: https://energyplus.net/weather (accessed on 4 May 2018).
40. ASHRAE. *ANSI/ASHRAE Standard 55-2004*; Thermal Environmental Conditions for Human Occupancy. American Society of Heating, Refrigerating and Air-Conditioning Engineers: Peachtree Corners, GA, USA, 2004.
41. ASHRAE. *ANSI/ASHRAE Standard 55-2013*; Thermal Environmental Conditions for Humman Occupancy. American Society of Heating, Refrigerating and Air-Conditioning Engineers: Peachtree Corners, GA, USA, 2013.
42. Marantos, C.; Siozios, K.; Soudris, D. Rapid Prototyping of Low-Complexity Orchestrator Targeting CyberPhysical Systems: The Smart-Thermostat Usecase. *IEEE Trans. Control Syst. Technol.* **2019**, *28*, 1831–1845. [CrossRef]
43. Nisan, N.; Roughgarden, T.; Tardos, E.; Vazirani, V. *Algorithmic Game Theory*; Cambridge University Press: Cambridge, UK, 2007. [CrossRef]
44. Osborne, M.J.; Rubinstein, A. *A Course in Game Theory*; The MIT Press: Cambridge, MA, USA, 1994.
45. Chatterjee, B. An optimization formulation to compute Nash equilibrium in finite games. In Proceedings of the 2009 International Conference on Methods and Models in Computer Science (ICM2CS), New Delhi, India, 14–15 December 2009; pp. 1–5.
46. Nash, J.F. Equilibrium points in n-person games. *Proc. Natl. Acad. Sci. USA* **1950**. *36*, 48–49. [CrossRef]
47. Lewis, R.; Torczon, V. Pattern Search Algorithms for Bound Constrained Minimization. *SIAM J. Optim.* **1999**, *9*, 1082–1099. [CrossRef]

48. Byrd, R.; Gilbert, J.; Nocedal, J. A trust region method based on interior point techniques for nonlinear programming. *Math. Program. Ser. B* **2000**, *89*, 149–185. [CrossRef]
49. Xilinx. Vivado High-Level Synthesis. 2018. Available online: https://www.xilinx.com/products/design-tools/vivado/integration/esl-design.html (accessed on 2 November 2024).